Contribution from the Departments of Chemistry, The Pennsylvania State University, University Park, Pennsylvania 16802, and The University of Colorado, Boulder, Colorado 80309

Rapid, Reversible Heterolytic Cleavage of the Co–Rh Bond in $(CO)_4Co$–$Rh(CO)(PEt_3)_2$

David A. Roberts,† William C. Mercer,† Gregory L. Geoffroy,*† and Cortlandt G. Pierpont‡

Received October 28, 1985

The complex $(CO)_4Co$–$Rh(CO)(PEt_3)_2$ (**1**) was prepared by the reaction of $Na[Co(CO)_4]$ with *trans*-$RhCl(CO)(PEt_3)_2$ and has been structurally characterized: $P2_1/c$, a = 8.294 (1) Å, b = 17.746 (6) Å, c = 16.575 (3) Å, β = 104.37 (1)°, V = 2363.2 (8) Å^3, Z = 4, R_1 = 0.042 and R_2 = 0.053 for 3209 reflections with $F > 6\sigma(F)$. The Co center is ligated by four carbonyls in an approximately tetrahedral arrangement while the Rh center has a square-planar arrangement of trans phosphines, a carbonyl, and the Co atom. The Co–Rh distance of 2.676 (1) Å is consistent with a single bond between these metals although the structural parameters and the reactivity properties of **1** imply that this is a polar donor–acceptor metal–metal bond between formally Co(−I) and Rh(+I) centers. The Co–Rh bond is readily cleaved by nucleophiles, and for example, addition of $[(Ph_3P)_2N]Cl$ to solutions of **1** gives immediate and quantitative formation of $[(Ph_3P)_2N]Co(CO)_4$ and *trans*-$RhCl(CO)(PEt_3)_2$. Even CH_3CN displaces this weak bond to form *trans*-$[Rh(CO)(PEt_3)_2(CH_3CN)]^+$ (**4**), and at low CH_3CN concentrations, the equilibrium **1** + CH_3CN ⇌ **4** + $[Co(CO)_4]^-$ is established. Variable-temperature NMR data indicate that the forward and reverse reactions in the above equilibrium are fast on the ^{31}P NMR time scale. Computer simulation of the NMR spectra has given the thermodynamic parameters for this equilibrium as well as rate and kinetic parameters for both the forward and reverse reactions. For illustration, the second-order rate constants for the forward and reverse reactions at 20 °C are 17 100 M^{-1} s^{-1} and 5.1 × 10^6 M^{-1} s^{-1}, respectively, corresponding to a turnover number of ~13 000/s for the equilibrium.

While polynuclear metal complexes offer the potential of giving unique chemistry as a consequence of the presence of adjacent metal centers, one of the well-recognized limitations of this class of compounds is the relative ease with which many fragment when placed under reaction conditions.[1] For example, CO readily fragments the tetranuclear clusters $H_2FeRu_3(CO)_{13}$ and $HCoRu_3(CO)_{13}$ to give $Ru_3(CO)_{12}$ and mononuclear Fe and Co carbonyls.[2] Most of the fragmentation reactions that have been reported are *irreversible* and as such would be clearly detectable in any attempts to use such compounds in catalytic reactions. However, *reversible* cluster fragmentation reactions might not be detectable under catalytic conditions if the rates of the reactions were rapid, and thus the fragmentation chemistry would cloud interpretation of the catalytic results. On the other hand, reversibility may be highly desirable if one wishes to use clusters as "storehouses" for catalytically active fragments.

In 1982, we communicated a unique case of a cleanly reversible fragmentation reaction with incredibly rapid rates of reaction, that involving the heterolytic cleavage of the polar Co–Rh bond in compound **1** when dissolved in the ligating solvent CH_3CN, eq 1.[3] We have since completed a detailed study of the reactivity

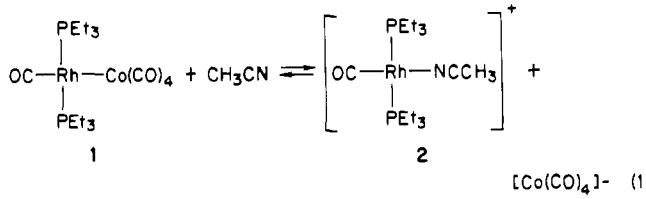

of this complex and report herein its complete characterization as well as equilibrium, thermodynamic, and kinetic parameters for the reactions given in eq 1.

Results

Synthesis and Spectroscopic Characterization of $(CO)_4Co$–$Rh(CO)(PEt_3)_2$ (1). The title complex results in high yield from reaction 2. The driving force for this reaction is the precipitation

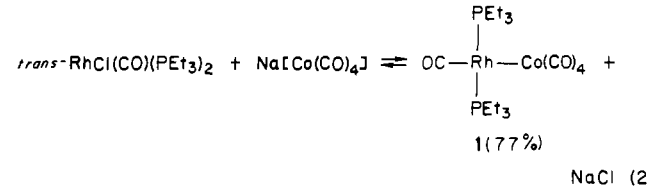

Table I. Selected Bond Angles and Distances in $(CO)_4Co$–$Rh(CO)(PEt_3)_2$ (**1**)

	Bond Distances (Å)		
Rh–Co	2.676 (1)	Co–C2	1.774 (7)
Rh–P1	2.346 (2)	Co–C3	1.770 (7)
Rh–P2	2.344 (2)	Co–C4	1.758 (7)
Rh–C1	1.811 (7)	Co–C5	1.769 (7)
Rh--C2	2.555 (8)		
Rh--C5	2.466 (6)		
	Bond Angles (deg)		
P1–Rh–P2	175.18 (5)	C2–Co–Rh	66.5 (2)
Co–Rh–C1	178.4 (2)	C2–Co–C3	103.0 (3)
C1–Rh–P1	87.13 (3)	C2–Co–C4	105.5 (4)
C1–Rh–P2	88.50 (3)	C2–Co–C5	129.1 (3)
Co–Rh–P1	87.1 (2)	C3–Co–Rh	131.8 (3)
Co–Rh–P2	88.5 (2)	C3–Co–C4	107.0 (3)
Co–C2–O2	169.4 (6)	C3–Co–C5	102.2 (3)
Co–C3–O3	177.7 (6)	C4–Co–Rh	121.1 (2)
Co–C4–O4	176.6 (6)	C4–Co–C5	108.3 (3)
Co–C5–O5	170.0 (7)	C5–Co–Rh	63.6 (2)

of NaCl, since the equilibrium constant for the reaction shown in eq 2 appears to be quite small. This is shown by experiments described below in which halide ions readily displace $[Co(CO)_4]^-$ from **1**. Complex **1** has been crystallographically characterized (Figure 1), and its spectroscopic data are consistent with the determined structure. Its $^{31}P\{^1H\}$ NMR spectrum shows a doublet at δ 16.8 (J(P–Rh) = 110 Hz), indicating the presence of two equivalent PEt_3 ligands bonded to a Rh(I) center. The 25 °C $^{13}C\{^1H\}$ NMR spectrum of **1** shows a singlet at δ 210.3 for the rapidly exchanging cobalt carbonyls and a doublet of triplets at δ 180.9 (J(C–Rh) = 80 Hz; J(C–P) = 16 Hz) for the Rh carbonyl.

Crystal and Molecular Structure of $(CO)_4Co$–$Rh(CO)(PEt_3)_2$ (1). An ORTEP drawing of complex **1** is shown in Figure 1, and relevant bond distances and angles are given in Table I. The geometry about the Rh center is square planar with trans phosphines, typical of most Rh(I) complexes containing two PR_3 ligands. The geometry about cobalt is best described as a distorted tetrahedron with the Rh center bisecting one tetrahedral edge. Carbonyl bond angles about the Co atom show only small deviations from tetrahedral values with the exception of the C2–Co–C5 bond angle, which has opened to 129.1 (3)° to accom-

† The Pennsylvania State University.
‡ The University of Colorado.

(1) Roberts, D. A.; Geoffroy, G. L In *Comprehensive Organometallic Chemistry*; Wilkinson, G., Stone, F. G., Abel, E. W., Eds.; Pergamon: Oxford, 1982; Vol. 6,.Chapter 40, pp 763–877.
(2) Steinhardt, P. C.; Gladfelter, W. L; Harley, A. D.; Fox, J. R.; Geoffroy, G. L. *Inorg. Chem.* **1980**, *19*, 332.
(3) Roberts, D. A.; Mercer, W. C.; Zahurak, S. M.; Geoffroy, G. L.; DeBrosse, C. W.; Cass, M. E.; Pierpont, C. G. *J. Am. Chem. Soc.* **1982**, *104*, 910.

0020-1669/86/1325-1439$01.50/0

modate the Rh center. The CO ligands that define this angle are slightly bent (Co–C2–O2 = 169.4 (2)° and Co–C5–O5 = 170.0 (5)°). Although these could be viewed as semibridging carbonyls,[4] the lack of significant carbonyl bending and the long Rh–C distances of 2.555 (8) and 2.466 (6) Å, as compared to the much shorter "normal" rhodium carbonyl carbon distance of 1.811 (7) Å for Rh–C1, indicate that this interaction is weak at best. Similar orientations of CO ligands have been observed for $[Co(CO)_4]^-$ bound to coordinatively unsaturated Pt and Pd centers.[5]

The Co–Rh bond distance of 2.676 (1) Å is consistent with the presence of a single bond between these metals by comparison to the Co–Rh distances in $Co_2Rh_2(\eta\text{-}C_5Me_5)_2(CO)_7$ (2.618 (3), 2.606 (4), 2.574 (4), 2.591 (3) Å[6a]) and on the basis of established Co–Ru single-bond distances (e.g., $[CoRu_3(CO)_{13}]^-$, Co–Ru = 2.618 Å (average);[2] $H_3CoRu_3(CO)_{12}$, Co–Ru = 2.675 Å[6b]) and Co–Pd single-bond distances (e.g., $CoPd(CO)_4(py)(C_{14}H_{13}N_2)$, Co–Pd = 2.604 (1) Å[5a]). It is 0.272 Å longer than the Co=Rh double-bond distance of 2.4040 (5) Å found in $RhCo(\eta\text{-}C_5H_5)_2(CO)_2$[6c] and is also nearly 0.1 Å longer than the 2.597 Å average Co–Rh single-bond distance in the above-mentioned $Co_2Rh_2(\eta\text{-}C_5Me_5)_2(CO)_7$ cluster.[6a] However, we believe the structural parameters imply that this bond in **1** is a donor–acceptor bond between formally Co(–I) and Rh(+I) centers (I) rather than

$$L_4Co \longrightarrow RhL_3$$

I

a covalent single metal–metal bond between Co(0) and Rh(0) centers. This conclusion is strongly supported by the geometries about the two metal centers. The observed square-planar geometry at Rh is typical of Rh(I) complexes. Indeed, complex **1** can be simply described as just another *trans*-$RhX(CO)(PR_3)_2$ derivative in which the donor ligand X is $Co(CO)_4$. The observed pseudotetrahedral arrangement of the carbonyl ligands on Co is also consistent with a d^{10} Co(–I) formulation for this metal. Also supporting the donor–acceptor formalism given to **1** are the reactions of the molecule discussed below in which heterolytic cleavage of the Co–Rh bond readily occurs with a variety of nucleophiles to give Rh(+I) products.

Displacement of the Rh–Co Bond in 1 by Halides. Halides readily displace the Co–Rh bond in **1** as illustrated by the quantitative reaction with [PPN]Cl shown in eq 3. Even NaCl

$$\underset{\mathbf{1}}{(CO)_4Co\text{-}Rh(CO)(PEt_3)_2} + [PPN]Cl \xrightarrow{THF} [PPN][Co(CO)_4] + \textit{trans}\text{-}RhCl(CO)(PEt_3)_2 \quad (3)$$

from IR-cell windows causes a similar reaction. The IR spectrum of **1** in THF solution when left in contact with the NaCl cell windows in the IR cell changed over the course of about 30 min to the spectrum characteristic of a mixture of *trans*-$RhCl(CO)(PEt_3)_2$ and $Na[Co(CO)_4]$. IR data obtained from the reaction of **1** with hydrogen chloride–dimethylacetamide (HCl·DMA), a convenient solid source of HCl, showed essentially quantitative formation of $HCo(CO)_4$ and *trans*-$RhCl(CO)(PEt_3)_2$. Likewise, the reaction of **1** with CH_3I led to a complicated mixture of products in which $CH_3Co(CO)_4$ and *trans*-$RhI(CO)(PEt_3)_2$ were identified as major constituents by their characteristic IR spectra.

Reaction of 1 with $CH_3O_2CC{\equiv}CCO_2CH_3$. Complex **1** showed no reaction with PhC≡CH or with PhC≡CPh. However, addition of $CH_3O_2CC{\equiv}CCO_2CH_3$ (DMAD) to hexane solutions

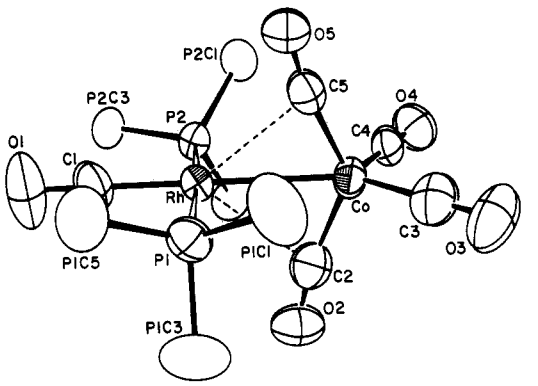

Figure 1. ORTEP drawing of $(CO)_4Co\text{-}Rh(CO)(PEt_3)_2$ (**1**). Only the PEt_3 carbons attached to phosphorus are drawn for clarity.

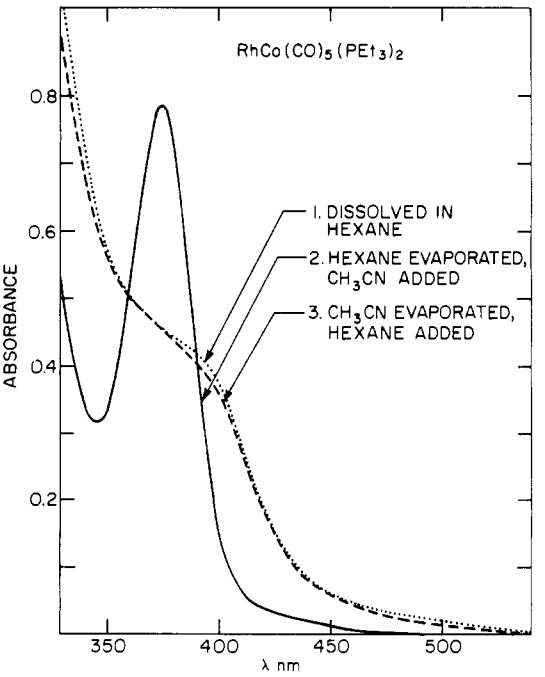

Figure 2. UV–visible spectra that result upon (a) dissolving **1** in hexane, (b) evaporating the hexane and adding CH_3CN, and (c) evaporating the CH_3CN and adding hexane.

of **1** gave an immediate precipitate in high yield of an orange powder for which an elemental analysis implies formulation as the 1:1 combination **1**·DMAD (eq 4). However, this material

$$\mathbf{1} + CH_3O_2CC{\equiv}CCO_2CH_3 \xrightarrow[\text{hexane}]{} \mathbf{1}\cdot CH_3O_2C{\equiv}CCO_2CH_3 \quad (4)$$

has proven difficult to characterize since it only forms when the reaction is conducted in hexane, and it decomposes to a complex mixture of products when dissolved in benzene, CH_2Cl_2, and other solvents. Although this compound may be a binuclear alkyne complex of some type, we believe that it is more likely the salt $[Rh(CO)(PEt_3)_2(DMAD)][Co(CO)_4]$ formed by the alkyne displacing the $[Co(CO)_4]^-$ fragment from **1** in a manner similar to that by halide ion as described above.

Rapid, Reversible Displacement of the Rh–Co Bond in 1 by CH_3CN. The nucleophilic solvent CH_3CN also displaces the Rh–Co bond in complex **1** to give the products shown in eq 5.

$$\underset{\mathbf{1}}{(CO)_4Co\text{-}Rh(CO)(PEt_3)_2} + CH_3CN \underset{k_r}{\overset{k_f}{\rightleftharpoons}} \textit{trans}\text{-}[OC\text{—}\underset{\underset{PEt_3}{|}}{\overset{PEt_3}{|}}Rh\text{—}NCCH_3]^+ + \underset{\mathbf{2}}{} [Co(CO)_4]^- \quad (5)$$

(4) Colton, R.; McCormick, M. J. *Coord. Chem. Rev.* **1980**, *31*, 1.
(5) (a) LeBorgne, G.; Bouaoud, S. E.; Grandjean, D.; Braunstein, P.; DeHand, J.; Pfeffer, M. *J. Organomet. Chem.* **1977**, *136*, 375. (b) Moras, D.; Dehand, J.; Weiss, R. *C. R. Seances Acad. Sci., Ser. C* **1968**, *267C*, 1471. (c) Braunstein, P.; Jud, J. M.; Dusausoy, Y.; Fischer, J. *Organometallics* **1983**, *2*, 180.
(6) (a) Braunstein, P.; Lehner, H.; Matt, D.; Tiripicchio, A.; Tiripicchio-Calmellini, M. *Nouv. J. Chim.* **1985**, *9*, 597. (b) Gladfelter, W. L.; Geoffroy, G. L.; Calabrese, J. C. *Inorg. Chem.* **1980**, *19*, 2569. (c) Green, M.; Hankey, D. R.; Hamond, J. A. K.; Lonca, P.; Stone, F. G. A. *J. Chem. Soc., Chem. Commun.* **1983**, 757.
(7) Brady, R.; Flynn, B. R.; Geoffroy, G. L.; Gray, H. B.; Peone, J., Jr.; Vaska, L. *Inorg. Chem.* **1976**, *15*, 1485.

Table II. Kinetic and Equilibrium Data for the Reaction of **1** with CH_3CN[a] (eq 5)

$CH_3CN/THF\text{-}d_8$[b]					CH_3CN/CD_2Cl_2[c]				
T, °C	k_{obsd}, s^{-1}	k_f, M^{-1} s^{-1}	k_r, M^{-1} s^{-1}	K_{eq}	T, °C	k_{obsd}, s^{-1}	k_f, M^{-1} s^{-1}	k_r, M^{-1} s^{-1}	K_{eq}
20	13000	17100	5.10×10^6	3.15×10^{-3}	45	7000	9280	1.33×10^6	6.99×10^{-3}
0	5600	7360	2.11×10^6	3.49×10^{-3}	23	4500	5970	8.03×10^5	7.43×10^{-3}
19	2200	2760	7.15×10^5	3.86×10^{-3}	−7	1400	1860	2.24×10^5	8.29×10^{-3}
42	650	855	1.69×10^5	5.05×10^{-3}	−40	255	340	4.03×10^4	8.43×10^{-3}
67	226	298	2.34×10^4	1.13×10^{-2}	−88	17	23	1.63×10^3	14.1×10^{-3}
93	16.5	22	7.48×10^2	2.94×10^{-2}					

[a] k_f and k_r values were calculated by assuming a second-order rate law, first order in both [**1**] and [CH_3CN]. [b] [**1**] = 0.0387 M; [CH_3CN] = 0.77 M. [c] [**1**] = 0.0219 M; [CH_3CN] = 0.77 M.

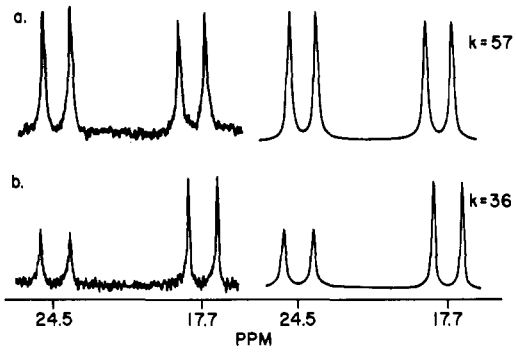

Figure 3. $^{31}P\{^1H\}$ NMR spectra of 2.2×10^{-3} M THF-d_8 solutions of **1** with CH_3CN added at concentrations of (a) 0.52 M and (b) 0.77 M.

When deep red **1** was dissolved in neat CH_3CN, a yellow solution resulted that contained only *trans*-$[Rh(CO)(CH_3CN)(PEt_3)_2]^+$ (**2**) and $[Co(CO)_4]^-$. Removal of the CH_3CN solvent regenerated hexane-soluble **1** in quantitative yield. Particularly illustrative are the UV–vis spectral changes shown in Figure 2 that were obtained during this experiment. Complex **1** shows a shoulder centered at ca. 390 nm that transforms into a sharp band at ca. 345 nm upon dissolution in CH_3CN. Such a band is characteristic of square-planar Rh(I) complexes[8] and is identical with that seen in the spectrum of an independent sample of **2**. The original spectrum of **1** reappears when the CH_3CN is evaporated from the cell and the residue dissolved in hexane.

When lesser quantities of CH_3CN are present in an inert solvent such as THF, both **1** and **2** exist in equilibrium. This is most clearly illustrated by the $^{31}P\{^1H\}$ NMR spectra shown in Figure 3, which were obtained at −80 °C at two different CH_3CN concentrations. Apparent are two doublets at δ 24.5 (J(P–Rh) = 110 Hz) and δ 17.7 (J(P–Rh) = 112 Hz), respectively, due to **2** and **1**, whose relative intensities clearly depend upon CH_3CN concentration. Equilibrium constants can be calculated from the integrated intensities for the two CH_3CN concentrations and are in quite good agreement: 1.2×10^{-4} (0.52 M) and 1.4×10^{-2} (0.77 M). Other weak bases are also capable of inducing heterolytic cleavage of the Co–Rh bond in **1**. Evidence for this comes from small but measurable conductivities obtained in acetone, THF, and CH_2Cl_2 solutions with respective values of Λ = 20.0, 0.1, and 0.2 M^{-1} Ω^{-1} cm^{-1}.

The variable-temperature $^{31}P\{^1H\}$ NMR spectra shown in Figure 4 show that the rates of the forward and reverse reactions involved in the equilibria of eq 5 are unusually rapid. At the lowest temperature recorded (−93 °C) resonances due to both **2** and **1** are apparent. As the temperature is raised, these resonances broaden, coalesce, and at 20 °C sharpen into a single doublet at δ 19.4 (J(P–Rh = 107 Hz), implying interconversion of **2** and **1** that is rapid on the NMR time scale. The spectral changes smoothly reverse upon cooling back to the low-temperature limit, showing that they are due to such an exchange process. Computer simulation of the spectra gave the rates for the exchange process and the equilibrium constants at the various temperatures, and these data are tabulated in Table II.

(8) Nixon, H. F. *Annu. Rep. NMR Spectrosc.* **1969**, *2*, 345.

Table III. Kinetic and Thermodynamic Data[a]

	CH_3CN/CD_2Cl_2	$CH_3CN/THF\text{-}d_8$
$\Delta H°$	−2.68 ± 0.33	−8.8 ± 2.9
$\Delta S°$	−49.8 ± 1.3	−82.4 ± 11.3
$\Delta G°$	12.2 ± 1.8	15.7 ± 6.3
ΔH_f	20.1 ± 2.5	21.3 ± 5.4
ΔS_f	−108.0 ± 9	−93.7 ± 28.5
ΔG_f	52.3 ± 5.2	49.2 ± 13.9
ΔH_r	22.7 ± 1.3	31.1 ± 7.5
ΔS_r	−56.1 ± 5.8	−7.8 ± 25.0
ΔG_r	39.4 ± 3.0	33.5 ± 15.0

[a] All parameters are for T = 298 K as standard state. Thermodynamic parameters are for the forward reaction of eq 5. Errors are given at 95% confidence limits. Units: ΔH and ΔG, kJ mol^{-1}; ΔS, J mol^{-1} K^{-1}.

Particularly informative are the computer simulations of the −80 °C spectra shown in Figure 3, which were recorded at the two different CH_3CN concentrations. The rate constants obtained are shown in the figure and they demonstrate that for this small set of data the rate of the exchange process is first order with respect to [CH_3CN] (eq 6). The rate constants obtained from

$$\text{rate} = k_f[\mathbf{1}][CH_3CN] \quad (6)$$

the computer simulation of the variable-temperature spectra shown in Figure 4 are then pseudo-first-order rate constants of the form

$$k_{obsd} = k_f[CH_3CN] \quad (7)$$

From the spectra shown in Figure 4, which were recorded with CH_3CN in large excess and hence with [CH_3CN] constant, the values of k_f, k_r, and K_{eq} were determined at each temperature. These data are also in Table II. The k_f and k_r values were determined under the assumption that the reaction is first order in both **1** and CH_3CN as noted above and from the relationships shown in eq 8–10. Qualitatively similar data (Table II) were

$$K_{eq} = [\mathbf{2}]^2/[\mathbf{1}][CH_3CN] \quad (8)$$

$$k_f = k_{obsd}/[CH_3CN] \quad (9)$$

$$k_r = k_f/K_{eq} \quad (10)$$

obtained from variable-temperature ^{31}P NMR spectra of **1** and CH_3CN dissolved in CD_2Cl_2 solution. Arrhenius and van't Hoff plots (supplementary material) gave the thermodynamic and kinetic parameters listed in Table III. The data were fit by a least-squares analysis with uncertainties in the derived parameters given to the 95% confidence limit.[21]

Reaction of 1 with $CH_3C(O)Cl$. The only reaction observed with complex **1** in which the Co–Rh bond was apparently maintained is with acetyl chloride. This gave the bimetallic oxidative-addition product **3** shown in eq 11. Complex **3** was isolated

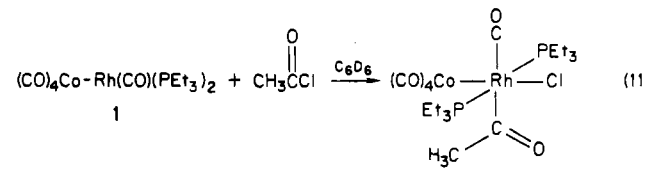

(11)

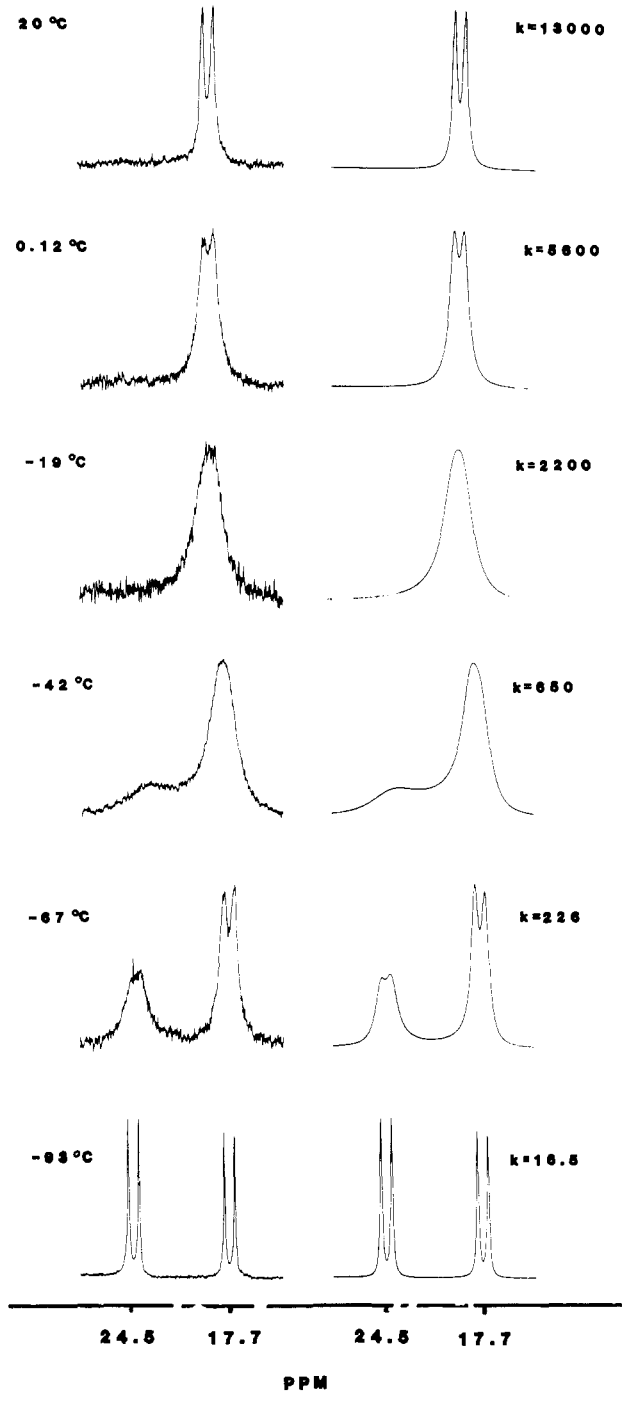

Figure 4. Variable-temperature ^{31}P NMR spectra for **1** dissolved in THF-d_8 that was also 0.77 M in CH_3CN. Experimental spectra with the acquisition temperatures are on the left, and computer-simulated spectra with first-order rate constants are on the right.

as an orange solid and was spectroscopically characterized. Its $^{31}P\{^1H\}$ NMR spectrum shows one doublet at δ 16.6, implying equivalent PR_3 ligands, and the decrease in the ^{31}P–^{103}Rh coupling constant in going from **1** (J = 110 Hz) to **3** (J = 90.6 Hz) is consistent with a conversion of a Rh(I) complex into a Rh(III) species since the latter generally show smaller ^{103}Rh–^{31}P couplings than do Rh(I) complexes.[8] Complex **3** also exhibited a characteristic acetyl ν(CO) stretch at 1602 cm^{-1}. Although the exact geometry of complex **3** is unknown, that drawn in eq 11 with the Cl and acetyl ligands in cis positions is assumed on the basis of the anticipated cis oxidative addition of acetyl chloride to **1**.

A small amount of *trans*-$RhCl(CO)(PEt_3)_2$ also forms during the reaction of eq 11. However, over the course of 16 h, the ^{31}P NMR resonance due to this species remained constant in relation to that of **3**. Formation of *trans*-$RhCl(CO)(PEt_3)_2$ was probably due to a small amount of HCl present in the acetyl chloride reagent.

Attempted Reaction of 1 with H_2. In an attempt to oxidatively add H_2 to **1**, the complex was allowed to stir for 6 h under H_2 pressure at 95 °C (1300 psi) and −20 °C (1100 psi). However, no significant reaction occurred since IR spectra of the solutions after opening the reactor showed mainly the presence of **1** along with a small amount (<5%) of unidentified compounds showing IR bands at 2020, 1994, 1987, 1812, and 1805 cm^{-1}. However, these same bands also appeared when solutions of **1** were allowed to stand in air for prolonged periods.

Discussion

The structural and chemical properties of complex **1** clearly indicate that it is best formulated as having a polar donor–acceptor bond between Co(−I) and Rh(+I) centers. It is thus a member of a growing family of compounds that have been formulated with similar donor–acceptor bonds, and as for many of these its chemistry is dominated by cleavage of this weak bond.[9] In the case of **1**, even weakly nucleophilic solvents such as CH_3CN will affect this reaction. As noted above, the reaction of **1** with CH_3CN is cleanly reversible and the rates of the reactions involved in the equilibrium of eq 5 are *unusually rapid*. The second-order rate constant for displacement of the $[Co(CO)_4]^-$ fragment by CH_3CN at 20 °C is 17 000 M^{-1} s^{-1} in THF solution (Table II), and the reverse reaction has a rate constant of 5.10×10^6 M^{-1} s^{-1} at this temperature. *We know of no other examples where rate constants for the cleavage and formation of metal–metal bonds have been measured and found to be so large.*[10] The results described herein clearly point to the difficulties that might be encountered when binuclear and polynuclear complexes such as **1** are used as homogeneous catalysts since the metal–metal bonds can be breaking and re-forming as fast as, if not faster than, the individual steps in the catalytic cycle. To illustrate this point more dramatically, *note that the rate of the* **1** *to* **2** *exchange process at 20 °C corresponds to a turnover number of 13 000/s.* This is far greater than turnover numbers of most homogeneous catalysts.

Displacement of $[Co(CO)_4]^-$ from the Rh center in **1** by CH_3CN is a ligand substitution reaction of a square-planar d^8 metal. In this reaction, the $[Co(CO)_4]^-$ fragment simply acts as a pseudohalide ligand, an analogy that has been previously noted for other compounds.[11] Ligand substitution reactions of square-planar complexes are well-known to obey a two-term rate law of the form given in eq 12 with competing solvent-assisted

$$\text{rate} = (k_1 + k_2[L])[\text{complex}] \qquad (12)$$

(k_1) and ligand-dependent (k_2) paths.[12] The rate of the reaction of **1** with CH_3CN was only measured at two different CH_3CN concentrations (Figure 3), but over this small data base the reaction shows a first-order dependence upon $[CH_3CN]$. Thus, contribution from the solvent-assisted path is minimal, even though the THF solvent molecules are potentially good ligands for Rh.

Valuable mechanistic and bond energy data can often be deduced from kinetic and thermodynamic data such as that obtained for the reaction of **1** with CH_3CN as summarized in Table III. The negative $\Delta H°$ value for the equilibrium in eq 5 implies that the Rh–$NCCH_3$ bond is stronger than the Rh–Co bond, but since

(9) (a) Einstein, F. W. B.; Pomeroy, R. K.; Rushman, P.; Willis, A. C. *Organometallics* **1985**, *4*, 250. (b) Einstein, F. W. B.; Jones, T.; Pomeroy, R. K.; Rushman, P. *J. Am. Chem. Soc.* **1984**, *106*, 2707. (c) Einstein, F. W. B.; Pomeroy, R. K.; Rushman, P.; Willis, A. C. *J. Chem. Soc., Chem. Commun.* **1983**, 854. (d) Barr, R. D.; Marder, T. B.; Orpen, A. G.; Williams, I. D. *J. Chem. Soc., Chem. Commun.* **1984**, 112. (e) Hames, B. W.; Legzdins, P. *Organometallics* **1982**, *1*, 116. (f) Meyer, T. J. *Prog. Inorg. Chem.* **1975**, *19*, 1.

(10) A related reversible fragmentation of the Pd–$Co(CO)_4$ bond in $PdMCo_2(CO)_7(dppm)_2$ (M = Pd, Pt) in Et_2O/THF solvents has been reported, but without quantification: Braunstein, P.; de Meric de Bellefon, C.; Ries, M. *J. Organomet. Chem.* **1984**, *262*, C14.

(11) Ellis, J. E. *J. Organomet. Chem.* **1975**, *86*, 1.

(12) (a) Basolo, F.; Pearson, R. G. *Mechanisms of Inorganic Reactions*; 2nd ed.; Wiley: New York, 1967. (b) Mureinik, R. J. *Coord. Chem. Rev.* **1978**, *25*, 1.

an accurate estimate of the former cannot be made, a quantitative value for the latter cannot be deduced. The large negative value of $\Delta S°$ (−81 J mol^{-1} K^{-1}) associated with this equilibrium is attributed to the increased solvation of the ionic products by the THF solvent molecules as the reaction proceeds in the forward direction. The significance of the activation parameters for the forward and reverse reactions of eq 5 is less certain because there must be significant, but unknown, changes in the degree of solvation as the reaction proceeds since neutral and ionic complexes are interconverted. However, the large negative ΔS value for the forward reaction in eq 5 (−90 J mol^{-1} K^{-1}) is consistent with the presumed associative nature of the reaction.

Experimental Section

The complex $[Rh(\mu\text{-}Cl)(CO)_2]_2$,[13] $Na[Co(CO)_4]$,[14] and *trans*-$RhCl(CO)(PEt_3)_2$ (**2**)[15] were prepared by literature procedures. The complex *trans*-$[Rh(CH_3CN)(CO)(PEt_3)_2]^+$ was generated in situ by addition of $AgPF_6$ to *trans*-$RhCl(CO)(PEt_3)_2$ in CH_3CN solution.[16] The reagents PEt_3 and $Co_2(CO)_8$ (Strem) and [PPN]Cl (PPN = $(Ph_3P)_2N^+$), $CH_3C(O)Cl$, PhC≡CPh, PhC≡CH, and $CH_3O_2CC{\equiv}CCO_2CH_3$ (Aldrich) were purchased and used as received. All manipulations were performed in standard Schlenk glassware under prepurified N_2 or in a nitrogen-filled drybox. Solvents were dried by stirring over Na/benzophenone (THF, hexanes, petroleum ether, benzene) or BaO (CH_2Cl_2) followed by distillation under N_2. NMR spectra were recorded on Bruker WP200, Bruker WM360, and JEOL PS100 FT-NMR spectrometers. $Cr(acac)_3$ (~1%) was added to each ^{13}C NMR sample as a shiftless relaxation agent.[17] ^{31}P NMR chemical shifts are relative to external H_3PO_4 with downfield chemical shifts reported as positive. Electron impact mass spectra were recorded on an AEI-MS9 mass spectrometer operated in the electron impact mode with a source voltage of 70 eV and probe temperatures in the 100–200 °C range. IR spectra were recorded on Perkin-Elmer 580 and IBM FT/IR-32 spectrometers. Elemental analyses were performed by Schwarzkopf Microanalytical Laboratory, Woodside, NY.

Preparation of $(CO)_4Co–Rh(CO)(PEt_3)_2$ (1). A THF (50-mL) solution of $Na[Co(CO)_4]$ (1.13 g, 5.80 mmol) was added to a THF (50-mL) solution of *trans*-$RhCl(CO)(PEt_3)_2$ (1.70 g, 4.22 mmol). The initial yellow solution became deep red. The solvent was removed in vacuo and the residue extracted with petroleum ether (65 mL). Concentration of the petroleum ether solution followed by cooling to −65 °C led to the deposition of orange-red crystals of **1** in 77% yield (1.75 g, 3.25 mmol). Anal. Calcd for $C_{17}H_{30}O_5P_2CoRh$: C, 37.92; H, 5.58. Found: C, 37.84; H, 5.80. IR (hexane): ν(CO) 2029 s, 1990 w, 1963 vs, 1953 vs, 1920 m, 1888 s cm^{-1}. $^{31}P\{^1H\}$ NMR (25 °C, C_6D_6): δ 16.8 (d, J(P–Rh) = 110 Hz), $^{13}C\{^1H\}$ NMR (25 °C, C_6D_6): δ 210.3 (br s, Co–CO), 180.9 (dt, Rh–CO, J(C–Rh) = 80 Hz, J(C–P) = 16 Hz). Mass spectrum: m/z 538 (M^+) and fragment ions corresponding to loss of 5 CO's.

Reaction of 1 with [PPN][Cl]. To a THF (30-mL) solution of **1** (0.050 g, 0.093 mmol) was added an excess of [PPN][Cl]. The solution immediately changed color from orange to pale yellow. The solvent was removed in vacuo and the residue extracted with hexane (30 mL). The IR spectrum of this solution showed a single IR absorption at 1957 cm^{-1} due to *trans*-$RhCl(CO)(PEt_3)_2$. The remaining residue was dissolved in CH_2Cl_2 (20 mL); its IR spectrum showed a single band at 1888 cm^{-1} due to $[PPN][Co(CO)_4]$.

Reaction of 1 with $CH_3C(O)Cl$. A C_6D_6 (1-mL) solution of **1** (0.050 g, 0.093 mmol) and $CH_3C(O)Cl$ (0.100 mL, 1.4 mmol) was prepared in a drybox and added to a 5-mm NMR tube. After 16 h of reaction, the ^{31}P NMR spectrum showed the major product to be $(CO)_4Co–Rh(C(O)CH_3)(Cl)(CO)(PEt_3)_2$ (**3**). The solvent was removed in vacuo, and the residue was chromatographed on SiO_2 (10% CH_2Cl_2/hexane) to yield first a yellow band of *trans*-$RhCl(CO)(PEt_3)_2$ (~10%) and then a second orange band of **3**, isolated in 40% yield (0.023 g, 0.037 mmol) by solvent evaporation. Anal. Calcd for $C_{19}H_{33}ClO_6P_2CoRh$: C, 36.98; H, 5.35. Found: C, 37.15; H, 5.20. $^{31}P\{^1H\}$ NMR (25 °C, C_6D_6): δ 16.6 (d, Rh–PEt_3, J(P–Ph) = 90.6 Hz). ^1H NMR (25 °C, C_6D_6): δ 1.67 (s, $C(O)CH_3$). IR (hexane): ν(CO) 2065 s, 2030 w, 1990 s, 1925 m, 189 m, 1602 w cm^{-1}. Mass spectrum: m/z 617 (M^+) and fragment ions corresponding to loss of 6 CO's and a CH_3 ligand.

Reaction of 1 with $CH_3O_2CC{\equiv}CCO_2CH_3$. To a solution of **1** (0.050 g, 0.093 mmol) in hexane (40 mL) was added $CH_3O_2CC{\equiv}CCO_2CH_3$ (DMAD; 0.11 mL, 0.093 mmol) via syringe. An immediate orange precipitate of **1**·DMAD formed and was isolated in 80% yield (0.050 g, 0.074 mmol) by filtration. Anal. Calcd for $C_{23}H_{36}O_9P_2CoRh$: C, 40.59; H, 5.29. Found: C, 40.51; H, 5.39. IR (KBr): ν(CO) 2046 s, 2015 vs, 1959 s, 1888 m, 1700 s br cm^{-1}.

Attempted Reaction of 1 with H_2. Solutions of **1** in hexane were placed in a 300-mL Parr Model 4753 stainless-steel pressure reactor and placed under the appropriate H_2 pressure. The solution was stirred at 85 °C (1300 psi) or −20 °C (1100 psi) for 6 h with the temperature maintained by the appropriate oil and slush baths. The pressure was released, and the contents were removed in an inert-atmosphere drybox. IR spectra showed mainly unreacted **1** with a small amount of other substances present giving IR bands at 2020, 1994, 1987, 1812, and 1805 cm^{-1}.

Reaction of 1 with HCl·DMA. The HCl adduct of dimethylacetamide (HCl·DMA), a convenient solid source of HCl, was prepared by bubbling HCl(g) through a solution of DMA to deposit a white precipitate of the adduct. To a CH_2Cl_2 solution of **1** (0.01 g, 0.019 mmol) was added HCl·DMA (0.003 g, 0.024 mmol). The solution immediately changed color from orange to yellow-green, and the IR spectrum showed that the ν(CO) bands of **1** had been replaced by the bands of $HCo(CO)_4$[18] and *trans*-$RhCl(CO)(PEt_3)_2$.

Variable-Temperature ^{31}P NMR Studies. Variable-temperature ^{31}P NMR spectra were obtained on Bruker WM360 and JEOL PS100 spectrometers. The temperature from −100 to +70 °C was maintained by a standard liquid-N_2-boil-off heat-exchanging apparatus with a thermal regulation of ±1 °C. Temperature measurements were obtained

Table IV. Crystal Data and Details of the Structure Determination for $(CO)_4Co–Rh(CO)(PEt_3)_2$ (**1**)

Crystal Data			
formula	$C_{17}H_{30}CoO_5P_2Rh$	vol, Å^3	2363.2 (8)
mol wt	538.14	Z	4
space group[a]	$P2_1/c$	d_{calcd}, g cm^{-3}	1.512
cryst syst	monoclinic	d_{exptl}, g cm^{-3}	1.50
a, Å[b]	8.294 (1)	F(000)	1096
b, Å	17.746 (6)	μ, cm^{-1}	15.63
c, Å	16.575 (3)	cryst dimens, mm	0.37 × 0.28 × 0.25
β, deg	104.37 (1)		

Data Collection and Reduction	
diffractometer	Syntex P1
data collcd	$\pm h,+k,+l$
radiation (γ, Å)	Mo Kα (0.710 69)
monochromator angle, deg	12.2
temp, K	294–296
scan technique	θ–2θ
scan range (2θ min–max), deg	3.0–50.0
scan speed, deg/min	4.0
scan range, deg	0.7 below Kα_1 and 0.7 above Kα_2
bkgd (scan time, s)	stationary crystal–stationary counter (0.5)
no. of unique reflcns measd	4323
no. of obsd reflcns	3209
criterion	$F > 6\sigma(F)$

Structure Determination and Refinement	
scattering factors	neutral atoms[c]
R_1, R_2[d]	0.042, 0.53
wt	$1/(\sigma^2(F) + 0.0005F^2)$
no. of params	235
ratio of observns to params	13.6
max shift/error (non-hydrogen atoms)	0.023
residual electron density, e/Å^3	1.8

[a] *International Tables for X-ray Crystallography*; Kynoch: Birmingham, England, 1965; Vol. 1. [b] Cell dimensions were determined by least-squares fit of the setting angles of 15 reflections with 2θ in the range of 20–30°. [c] *International Tables for X-ray Crystallography*; Kynoch: Birmingham, England, 1974; Vol. 4, pp 55–60, 99–101, 149–150. [d] The quantity minimized in the least-squares procedure is $\sum w(|F_o| - |F_c|)^2$. $R_1 = \sum||F_o| - |F_c||/\sum|F_o|$; $R_2 = [\sum w(|F_o| - |F_c|)^2/\sum w|F_o|^2]^{1/2}$.

(13) Cramer, R. *Inorg. Synth.* **1974**, *15*, 14.
(14) Ruff, J. K.; Schlientz, W. J. *Inorg. Synth.* **1974**, *15*, 84.
(15) Prepared by adding 4 equiv of PEt_3 to 1 equiv of $Rh_2(\mu\text{-}Cl)_2(CO)_4$ in hexane under N_2. See: Chatt, J.; Shaw, B. L. *J. Chem. Soc. A* **1966**, 1437.
(16) Heras, J. V.; Pinilla, E.; Oro, L. A. *Transition Met. Chem. (Weinheim, Ger.)* **1981**, *6*, 45.
(17) Gansow, O. A.; Burke, A. R.; LaMar, G. N. *J. Chem. Soc., Chem. Commun.* **1972**, 456.
(18) Sternberg, H. W.; Wender, I.; Friedel, R. A.; Orchin, M. *J. Am. Chem. Soc.* **1953**, *75*, 2717.

Table V. Atomic Positional and Isotropic Thermal Parameters for $(CO)_4Co-Rh(CO)(PEt_3)_2$ (**1**)

atom	*x*	*y*	*z*	*B*, Å^{2a}
Rh	−0.22714 (5)	0.13850 (2)	0.16219 (3)	3.13 (2)
Co	0.04641 (9)	0.21851 (5)	0.16668 (5)	3.51 (4)
P1	−0.0911 (2)	0.05308 (8)	0.26461 (9)	3.92 (7)
P2	−0.3793 (2)	0.21581 (8)	0.05553 (9)	3.52 (6)
P1C1	0.0840 (10)	0.0879 (4)	0.3470 (5)	5.8 (4)
P1C2	0.1714 (11)	0.0289 (5)	0.4136 (5)	6.8 (5)
P1C3	0.0017 (11)	−0.0265 (4)	0.2225 (5)	6.6 (4)
P1C4	−0.1206 (13)	−0.0659 (5)	0.1498 (6)	8.1 (5)
P1C5	−0.2273 (10)	0.0075 (5)	0.3229 (5)	6.4 (4)
P1C6	−0.3026 (12)	0.0655 (6)	0.3741 (6)	9.2 (6)
P2C1	−0.3746 (8)	0.3176 (3)	0.0754 (4)	4.9 (3)
P2C2	−0.4623 (10)	0.3404 (5)	0.1449 (5)	6.6 (4)
P2C3	−0.6037 (7)	0.1930 (4)	0.0247 (4)	4.1 (3)
P2C4	−0.7097 (9)	0.2414 (5)	−0.0438 (4)	5.8 (4)
P2C5	−0.3152 (8)	0.2110 (4)	−0.0439 (4)	4.9 (3)
P2C6	−0.3413 (10)	0.1316 (5)	−0.0812 (4)	6.5 (4)
C1	−0.4148 (8)	0.0842 (4)	0.1560 (4)	4.9 (3)
O1	−0.5356 (7)	0.0499 (3)	0.1533 (4)	8.7 (3)
C2	0.0273 (9)	0.1381 (4)	0.1013 (4)	5.0 (3)
O2	0.0364 (7)	0.0895 (3)	0.0566 (4)	7.8 (3)
C3	0.2544 (9)	0.2103 (4)	0.2291 (4)	5.2 (3)
O3	0.3877 (6)	0.2065 (4)	0.2670 (3)	7.4 (3)
C4	0.0449 (8)	0.2963 (4)	0.1005 (4)	4.4 (3)
O4	0.0509 (7)	0.3477 (3)	0.0591 (3)	6.7 (3)
C5	−0.0636 (8)	0.2426 (3)	0.2410 (4)	4.3 (3)
O5	−0.1185 (6)	0.2659 (3)	0.2946 (3)	6.0 (3)

[a] Hamilton, W. C. *Acta Crystallogr.* **1959**, *12*, 609.

by using a sample of PPh_3/PPh_3O in toluene-d_8 as a ^{31}P thermometer.[19] The spectrum for this solution was recorded before and after the data acquisition for each sample at each temperature. All solutions were allowed to thermally equilibrate in the probe at a given temperature for at least 15 min. Samples were prepared in a drybox in 10-mm NMR tubes with ground-glass joints attached. These were transferred under N_2 to a vacuum line where they were degassed and sealed with a torch. The samples were kept frozen in liquid N_2 when not in the spectrometer to minimize decomposition. For the dynamic NMR study of **1** in CH_3CN, 4.00 ± 0.05 mL of THF-d_8 was added to 0.0867 g of **1** via syringe. To 3.15 mL of this solution was added 0.15 mL of CH_3CN. The tube was then capped and sealed under vacuum. Relaxation measurements at −80 °C established that both **1** and *trans*-$[Rh(CO)(CH_3CN)(PEt_3)_2]^+$ have $T_1 = 0.81 \pm 0.09$. This eliminates the need for long delay times during data acquisition. Values of T_2^* were estimated from half-height line widths for samples of **1** prior to CH_3CN addition. Once obtained, the variable-temperature spectra were simulated by the program DNMR3.[20] Values for $\Delta H°$, $\Delta S°$, ΔH, ΔS, and ΔG were respectively determined from plots of K_{eq} vs. $1/T$ and k_1 vs. $1/T$ and are expressed with 298 K as the standard temperature at 95% confidence limits.[21]

X-ray Structure Determination of $(CO)_4Co-Rh(CO)(PEt_3)_2$ (1). Deep red crystals of **1** were grown from a saturated petroleum ether solution at −65 °C. A suitable crystal was mounted on an automated diffractometer, and cell constants were obtained from the refined settings of 15 reflections with 2θ settings greater than 20° (Mo Kα radiation). ψ scans on reflections near $\theta = 90°$ indicated only random fluctuations, so an empirical absorption correction was not carried out. Pertinent crystal and intensity data are given in Table IV. The computer programs and calculational procedures used in this study have been previously described.[22] The locations of the Rh and Co atoms were obtained from a Patterson map, and the remaining atoms were located with phases from these atoms. The hydrogen atoms of the PEt_3 ligands were placed in calculated positions ($d = 0.98$ Å) but were not refined. The structure smoothly converged to $R = 0.042$ and $R_w = 0.053$ upon least-squares refinement using anisotropic thermal parameters for all non-hydrogen atoms. Atomic positional parameters are given in Table V, and thermal parameters and structure factors are included in the supplementary material.

Acknowledgment. This research was supported by the National Science Foundation (Grant CHE8201160). Johnson-Matthey, Inc., is gratefully acknowledged for the loan of the Rh salts. Susan Zahorak and Charles deBrosse are also acknowledged for experimental assistance.

Registry No. **1**, 81048-71-7; **3**, 101375-17-1; $[Rh(CO)(PEt_3)_2(DMAD)][Co(CO)_4]$, 101349-48-8; *trans*-$RhCl(CO)(PEt_3)_2$, 15631-52-4; [PPN][$Co(CO)_4$], 53433-12-8; $Na[Co(CO)_4]$, 14878-28-5; $HCo(CO)_4$, 16842-03-8; $CH_3C(O)Cl$, 75-36-5; Rh, 7440-16-6; Co, 7440-48-4.

Supplementary Material Available: Tables of anisotropic temperature parameters and structure factors for **1** and Arrhenius and van't Hoff plots for the variable-temperature ^{31}P NMR study of the reaction of **1** with CH_6CN (16 pages). Ordering information is given on any current masthead page.

(19) Dickert, F. L.; Hellmann, S. W. *Anal. Chem.* **1980**, *52*, 996.
(20) Bench, G.; Kleier, D. A. Program No. 165, Quantum Chemistry Program Exchange, Indiana University, Bloomington, IN.
(21) Draper, N. R.; Smith, H. *Applied Regression Analysis*; Wiley: New York, 1966.
(22) Pierpont, C. G. *Inorg. Chem.* **1977**, *16*, 636.